

## Medium-Range Order in Silica, the Canonical Network Glass

P. H. Gaskell and D. J. Wallis\*

*Cavendish Laboratory, University of Cambridge, Madingley Road, Cambridge CB3 0HE, United Kingdom*

(Received 11 August 1995)

Most of the diffraction data for silica, the prototypical network glass, can be understood through local structural parameters. Failures to fit the prominent first (sharp) diffraction peak (FSDP), giving vital clues to medium-range order, are spectacular, however. We show a correspondence between FSDPs in glasses and crystals and examine anisotropic scattering from atomic models for  $\alpha$ -SiO<sub>2</sub>. The FSDP is related to quasi-Bragg planes, specified by features to  $\sim 1$  nm in the correlation function, thus defining the medium-range structure. Arguments are general, applicable to most amorphous materials.

PACS numbers: 61.43.-j, 61.10.Dp, 61.12.-q, 61.16.-d

First sharp diffraction peaks (FSDPs) are seen in a wide range of glasses from framework structures like silica, to close-packed amorphous alloys, molecular glasses, and even melts at high temperatures [1]. The temperature dependence of the peak intensity may be anomalous—increasing with temperature [2], although it is not clear that this behavior is general. In silica glass, neutron-induced disorder causes the peak to become significantly weaker [3,4]. One of the more surprising features, the generality of which has not been emphasized in earlier work, is that the position of the first peak corresponds closely to that of a strong diffraction peak in a related crystalline phase and, therefore, to associated Bragg planes (Table I). We believe this to be a most important clue to the origin of the FSDP. Although *layers*, similar to two-dimensional layers of the corresponding crystals, have been postulated as the origin of FSDPs in chalcogenide glasses [2], the concept of layers in tetrahedral, framework glasses is much less palatable. Indeed, the presence of a FSDP for silica and the three dimensionality of its structure have been used as arguments to discredit a possible general explanation in terms of atomic layers. For a review of alternative explanations, see Elliott [5].

We propose that quasilattice planes in glasses (as distinct from two-dimensional layers) analogous to Bragg planes in compositionally equivalent crystals, reveal the origin of the FSDP in silica and, by extension, in other glasses.

We have investigated this hypothesis by examining *anisotropic* scattering from atomic models of amorphous silica ( $\alpha$ -SiO<sub>2</sub>). The simulated scattered intensity from relatively small disordered atomic models depends on the orientation of the model in relation to the incident and scattered wave vectors  $\mathbf{Q}_i$  and  $\mathbf{Q}_s$ . The intensity scattered from a microcrystallite would be nonzero for a set of “Bragg” orientations only: For a disordered solid, fluctuations in order that *resemble* Bragg planes produce a scattered intensity greater than the mean and, as in crystals, planes are oriented normal to the scattering vector  $\mathbf{Q} = \mathbf{Q}_i - \mathbf{Q}_s$ . We can thus select orientations corresponding to high, medium, and low values of the anisotropic scattered intensity  $I(\mathbf{Q})$  for values of  $Q = |\mathbf{Q}| = Q_1 = 15.2 \text{ nm}^{-1}$ , the position of the FSDP. The

corresponding projections of the model normal to  $\mathbf{Q}$  then provide clues to the origin of the FSDP.

We consider spherical cores ( $\sim 700$  and  $1600$  atoms, respectively) cut from  $1000$ - and  $2000$ -atom models constructed by Gladden [6] and the  $3000$ -atom model of Wicks [7]. These models provide a good fit to the experimental diffraction data [8]—including the position, intensity, and breadth of the FSDP—and are unusual in this respect. We have ignored similar models which conflict with other properties of silica (one contains an unphysical proportion of three-membered rings).

We have calculated the orientation-dependent intensity  $I(\mathbf{Q})$  with  $Q = Q_1$  corresponding to the first peak of the orientationally *averaged* scattered intensity.  $\mathbf{Q}_{\max}$ , corresponding to the maximum intensity  $I_{\max}(\mathbf{Q})$ , was selected and a projection of the model plotted normal to  $\mathbf{Q}_{\max}$ . For a microcrystallite, this would show Bragg planes with a spacing  $d_1 = 2\pi/Q_1$ . In some models for  $\alpha$ -SiO<sub>2</sub>, planes with a spacing  $d_1 = 0.4$  nm are recognizable, though they are diffuse and ill-defined. Figure 1(a) is a projection, corresponding to  $\mathbf{Q}_{\max}$ , of the atomic coordinates of Gladden’s  $1000$ -atom model. Figure 1(b) shows another representation in the form of a simulated high resolution electron microscope (HREM) image. Parameters chosen provide a faithful representation of the atomic density, and again planes are clearly visible. A simulated microdiffraction pattern (not shown) contains a pair of diffraction spots normal to the planes and a weaker pair corresponding to planar features running from top left to bottom right in Figs. 1(a) and 1(b). For orientations corresponding to the average scattered intensity, corresponding to  $I(\mathbf{Q}) \approx \bar{I}(Q)$ , planes are much less distinct [Fig. 1(c)].

Some planar features are also seen in Figs. 1(d) and 1(e) for Gladden’s  $2000$ -atom model [6] and (less convincingly) in the  $3000$ -atom model of Wicks [7]. Planes corresponding to  $\mathbf{Q}_{\max}$  for some of the (many) models that give poor representations of the FSDP are similar to Fig. 1(c) and exhibit no obvious ordering.

The relative probability of maximal values of the normalized scattered intensity  $I_{\max}^* = I_{\max}(\mathbf{Q})/\bar{I}(Q_1)$  has been calculated following the prescriptions of Alben, Cargill, and Wenzel [9]. They showed that if  $I^* = I(\mathbf{Q})/$

TABLE I. Comparison of the position  $Q_1$  of the first sharp diffraction peak in several types of glass (upper part) and liquid with ( $2\pi/d_{\text{cryst}}$ ) where  $d_{\text{cryst}}$  is the lattice spacing for the first peak (generally) in the x-ray diffraction data for compositionally similar crystals. On the whole the correspondence is good, although there are notable exceptions—such as  $\text{B}_2\text{O}_3$ .

	$Q_1$ ( $\text{nm}^{-1}$ )	$2\pi/d_{\text{cryst}}$ ( $\text{nm}^{-1}$ )	Crystal phase
$\text{SiO}_2$	15.2	15.5	Cristobalite
		15.3	Tridymite
$\text{GeO}_2$	15.5	15.4	Cristobalite
$\text{B}_2\text{O}_3$	15.8	22.5	Hex. (high press.)
		10.3, 19.6	Cub. (high press.)
$\text{BeF}_2$	16.3	16.0	Cristobalite-type
$\text{GeS}_2$	10.4	11.0	High temp. mod.
$\text{GeSe}_2$	10.1	10.6	High temp. mod.
$\text{As}_2\text{S}_3$	12.8	12.7	
$\text{ZnCl}_2$	10.8	12.8	(Devit. glass)
		10.2; 11.7; 11.4	$\beta$ ; $\gamma$ ; $\delta$
$\text{Li}_2\text{Si}_2\text{O}_5$	17.3	17.4	
$\text{Na}_2\text{Si}_2\text{O}_5$	18.3	16.2	
$\text{CaSiO}_3$	20.2	21.1	Wollastonit-2M
$\text{SrSi}_2\text{O}_5$	20.4	19.2	Metastable <i>c</i> - $\text{SrSiO}_3$
		21.7	Stable <i>c</i> - $\text{SrSiO}_3$
$\text{LiAlSi}_2\text{O}_6$	16.1	18.0	$\beta$ spodumene
l- $\text{ZnCl}_2$	10.1	10.2; 11.7; 11.4	$\beta$ ; $\gamma$ ; $\delta$
l- $\text{ZnBr}_2$ (693 K)	9.4	10.0	(25 kbar)
l- $\text{ZnI}_2$ (743 K)	8.8	9.0	
l- $\text{NiCl}_2$	9.9	10.9	
l- $\text{NiBr}_2$	9.2	10.3	
l- $\text{NiI}_2$	8.8	9.6	

$\bar{I}(Q) > 2\ln(QV^{1/3}) + 0.5$ , the probability is  $<0.1$  that the scattered intensity results from a random atomic arrangement. ( $V$  is the volume of the model.)  $I_{\text{max}}^*$  for the three models shown in Figs. 1(a), 1(d), and 1(e) are 9.9 (7.5), 10.5 (8.1), and 8.4 (8.0); values in brackets are those calculated for *random scatterers*. The first two models (Gladden) appear to contain significant order, the third (Wicks) is somewhat marginal: Others, not fitting the FSDP, have lower  $I_{\text{max}}^*$  values, giving no indication of ordering exceeding that for random models. Specifically,  $I_{\text{max}}^*$  values are about (80–95)% of the “maximum” value for random scatterers, as are values of  $I_{\text{max}}^*$  calculated for all models, successful or not, for the second diffraction peak ( $Q_2 = 30 \text{ nm}^{-1}$ ), which can be represented more adequately by short-range correlations.

The distribution of normalized intensities  $I^*$  shows that for models where  $I_{\text{max}}^*$  exceeds the value calculated for random scatterers, the *variance* is also large compared to the cases where  $I_{\text{max}}^*$  is relatively small. Moreover, the distribution has a characteristic excess (compared to random scatterers) at high values of  $I^*$ , with a corresponding decrease at lower values of  $I^*$ . This is exactly the behavior expected as atomic density oscillations become more pronounced (in the limit, tending towards a microcrystallite). This may explain in part the high values of  $\bar{I}(Q_1)$  for successful models. There is the further effect that increasing order emphasizes the sharpening of the FSDP and there is some evidence for this: The intensity in the wings is lower for successful models.

HREM provides a two-dimensional representation of the projected atomic potential and, in principle, images planes of high atomic density directly [10]. Figure 1 compares a typical experimental micrograph with simulated HREM images. While scattering data support the notion that planelike fluctuations in atomic density lie at the heart of an explanation of FSDPs, scattering data alone give little direct evidence of their spatial extent, the degree of curvature [11], parallelism, etc. HREM images, despite the difficulties (and in the past, controversies) over interpretation, offer such evidence.

Do the planes have any of the characteristics of crystalline  $\text{SiO}_2$ ? The period is approximately 0.41 nm, close to values for  $\beta$ -cristobalite ( $\{111\}$  planes at 0.411 nm).  $\beta$ -cristobalite is approximately a diamond-cubic Si lattice with O midway between Si.  $\{111\}$  planes are puckered arrangements of Si and O, with each plane connected to its neighbor by further oxygens along  $\langle 111 \rangle$ . For the planes to be really “*cristobalite* quasilattice planes” a high proportion of O and Si lying on  $\{111\}$  planes will be connected, with a significant number of oxygens between the planes (on “*antiplanes*”) bonded across them. The connectivity in Gladden’s 2000-atom model (which gives the highest  $I^*$  value) was examined by selecting atoms giving positive contributions to the scattering amplitude. Projections of two adjacent planes are shown in Fig. 2(a). Atoms clearly have higher *in-plane* connectivity than those on adjacent “*antiplanes*,” Fig. 2(b). In this regard at least, the structure mimics  $\{111\}$  planes of  $\beta$ -cristobalite.

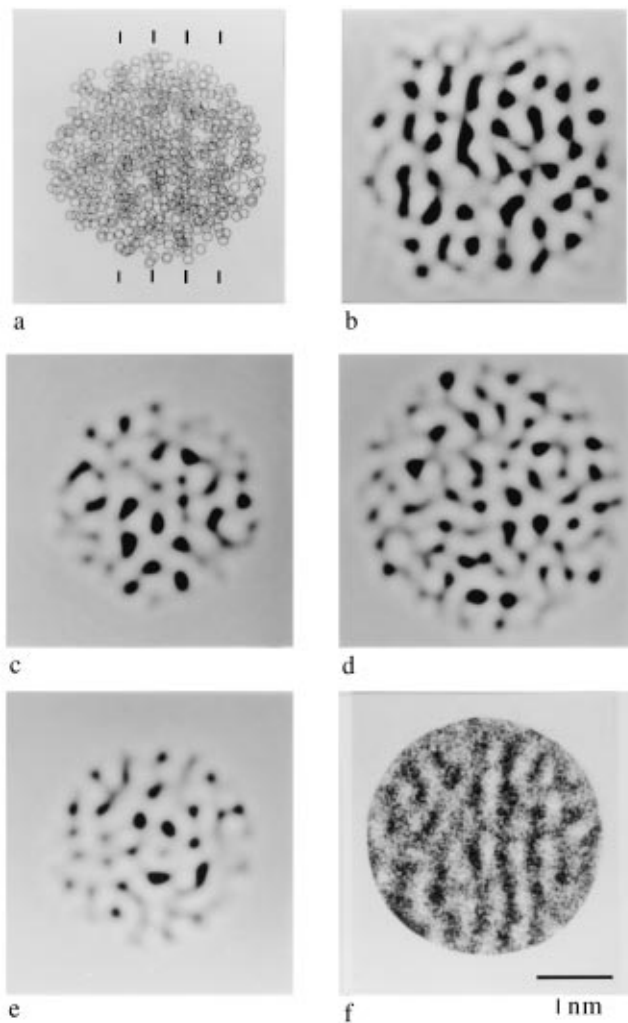


FIG. 1. (a) Projection of part of a 1000-atom model of silica constructed by Gladden [6], orientated so that the strongest scattering vector  $\mathbf{Q}_{\max}$  lies along the abscissa and the projected planes are parallel to the ordinate. The planes are made more visible by tilting the diagram and viewing at an oblique angle parallel to the ordinate. Markers have been added at intervals of 0.41 nm as a guide to the eye. (b) Simulated HREM image of the projection shown in (a). The image was produced by a multislice program ("Cerius 2") and includes corrections for instrumental aberrations under typical experimental operating conditions. [Electron energy 200 kV, spherical aberration constant  $C_s = 0.52$  mm, defocus  $-40$  nm (corresponding to Scherzer defocus), focal spread 8.4 nm, and beam divergence 1.0 mrad.] Images generated under these conditions give a good representation of fluctuations in atomic density and minimize image artifacts that are not specimen dependent. (c) Simulated image for the same model orientated so that  $I(\mathbf{Q})$  corresponds to the average intensity  $\bar{I}$ . In this case, planes are not recognizable. (d),(e) HREM images for part of Gladden's 2000-atom model [6] and Wicks' 3000-atom model [7], respectively. In each case the strong scattering direction is arranged to give planes parallel to the ordinate. (f) An experimental high resolution electron microscope image of amorphous  $\text{SiO}_2$  with imaging conditions similar to those mentioned in (b).

A further controversy surrounds the quantitative and qualitative explanations of the representation of FSDPs in real space data. Where in the one-dimensional real space

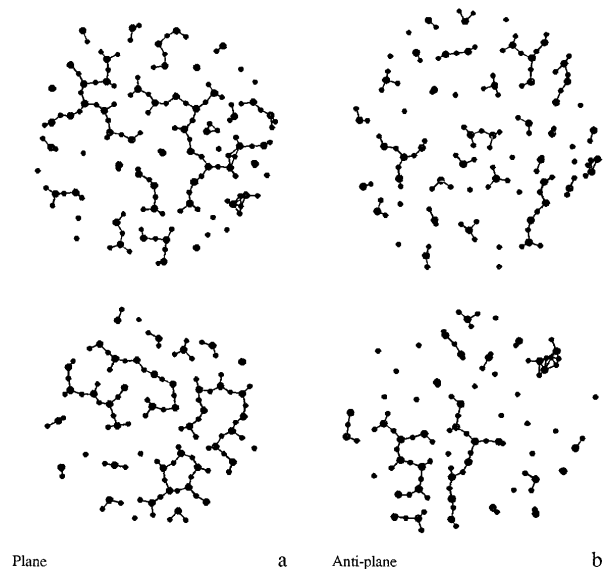


FIG. 2. The connectivity of atoms in Gladden's 2000-atom model for silica [6]. The structure has been partitioned into quasilattice planes and "antiplanes" as described in the text. Atoms lying on planes (a) (defined as those giving a positive contribution to the phase of the scattered amplitude) are more extensively connected to other atoms on the same plane compared to those lying on intermediate antiplanes (b). Note the presence in this model of atoms that are unphysically close to each other.

correlation function  $G(r)$  are the features "stored" that produce FSDPs in reciprocal space? Previous explanations have stressed oscillations in  $G(r)$  [12], extending perhaps to 2–4 nm [13]. Others argue for a particular strong feature in  $G(r)$ , or clusters on the scale of the medium-range order. Here we link the FSDP to "quasi-Bragg" planes, homologous with (real) Bragg planes and therefore proceed from an understanding of crystal diffraction.

At the Bragg condition, a lattice is effectively partitioned into planes normal to  $\mathbf{Q}_{hkl}$  with a separation  $d_{hkl} = 2\pi/Q_{hkl}$ . Atoms on these planes scatter in phase, and with a phase difference,  $\exp(i\mathbf{Q}_{hkl} \cdot \mathbf{r}_i)$ , otherwise. Atoms are specified by vectors  $\mathbf{r}_i$  whereas the pair correlation function  $G(r)$ , averaged over all orientations, is expressed in terms of scalars  $r_{ij}$ . There is no requirement for *any*  $r_{ij}$  to correspond to  $d_{hkl}$ . But Bragg planes *are* specified by a *set* of scalar interatomic distances. That is, the specification for  $d_{hkl}$  is contained in the *conjunction* of  $r_{ij}$  values appropriate to the structure. [Just as the  $\text{SiO}_4$  tetrahedron is specified by the set of four equal Si-O distances  $R$  and 6 O-O distances at  $(2/3)^{1/2}R$ .] The  $\{111\}$  planes in  $\beta$ -cristobalite are represented by the conjunction of 1- to  $n$ -neighbor Si-O distances with corresponding distances and coordination numbers for other atom pairs. Similarly, it is the conjunction of these features in  $G(r)$  which encodes the position, shape, and intensity of the FSDP in  $\alpha$ - $\text{SiO}_2$ . (It should be stressed perhaps that a real space signature for the FSDP in  $\text{SiO}_2$  in the form of a decaying sinusoid of period  $2\pi/Q_1$  is only *conditionally* correct: for example, when the first peak is (artificially)

separated from the rest of the diffraction data. We consider this approach to have limited generality and, in the case of silica, to be misleading.

Which part of  $G(r)$  contains the essential information that specifies the FSDP? Figure 3 shows diffraction data for  $\alpha$ -SiO<sub>2</sub> obtained by neutron scattering [14] which has been Fourier transformed to  $G(r)$ , then truncated at several values  $R_{\max}$ , and finally backtransformed into reciprocal space. For  $R_{\max} = 0.46$  nm, the FSDP is recognizable but far too broad. For  $R_{\max} > 1$  nm, the FSDP is scarcely distinguishable from the original data or from the transform to 4 nm. This shows, with little ambiguity, that a structure consistent with the FSDP can be specified by a pair correlation function extending to values of  $r \approx 1$  nm, a value similar to the correlation length 1.2–1.35 nm, estimated by Salmon [12]. Longer-range fluctuations in atomic density characteristic of “extended range correlations” [12] are of little importance.

In summary, we have tried to characterize the structure of  $\alpha$ -SiO<sub>2</sub> by interpreting the first diffraction peak and have shown that anisotropic scattering is directly related to the prominence of periodic fluctuations in atomic density—“quasiBragg planes.” Prominent planes are seen in models that give a good fit to the FSDP, thus revealing the origin of this feature of the diffraction data. Atomic density fluctuations correspond to a reasonably well-defined interplanar spacing which, in turn, is defined by particular conjunc-

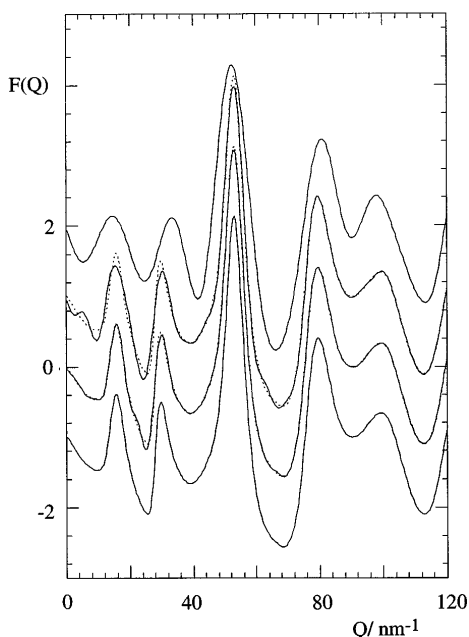


FIG. 3. Fourier transforms  $F(Q) = Q[S(Q) - 1]$  of the reduced pair correlation function  $G(r)$  for silica obtained by a transform of experimental neutron scattering data [12] [modified by multiplication with a function of the type  $\sin(\zeta)/\zeta$  where  $\zeta = \pi Q/Q_{\max}$ , chosen to avoid artifacts (ripples in  $r$  space) associated with truncation at several values  $R_{\max}$ , chosen as even nodes of  $G(r)$ ]. From top to bottom:  $R_{\max}$  is 0.46, 0.83, 1.07, and 4.0 nm. Experimental  $F(Q)$  data are shown as the dotted line superimposed on the lower three plots. Each  $F(Q)$  plot is displaced by 1.0 for clarity.

tions of 1- to  $n$ -neighbor spacings ( $n \sim 6$ ), corresponding coordination numbers, and the mean atomic density.

We are grateful to Dr. Lynn Gladden and Dr. Jim Wicks for valuable discussions and for providing atomic coordinates. Constructive comments from Dr. Gavin Mountjoy have proved extremely helpful. D.J.W. acknowledges the support of SERC through a CASE studentship with Pilkington plc. P.H.G. is grateful to Professor Georges Calas for useful discussions and generous hospitality and to CNRS for support for a sabbatical period in the Universit es Pierre et Marie Curie, Paris 7, where some of this work was carried out.

\*Present address: Oak Ridge National Laboratory, Solid State Division, P.O. Box 2008, Oak Ridge, TN 37831-6030.

- [1] D. A. Allen, R. A. Howe, N. D. Wood, and W. S. Howells, *J. Chem. Phys.* **94**, 5071–5076 (1991).
- [2] L. E. Busse and S. R. Nagel, *Phys. Rev. Lett.* **47**, 1848 (1981); L. E. Busse, *Phys. Rev. B* **29**, 3639 (1984).
- [3] S. Susman, K. J. Volin, D. L. Price, M. Grimsditch, J. P. Rino, R. K. Kalia, P. Vashishta, G. Gwanmesia, Y. Wang, and R. C. Liebermann, *Phys. Rev. B* **43**, 1194–1197 (1991).
- [4] A. C. Wright, B. Bachra, T. M. Brunier, R. N. Sinclair, L. F. Gladden, and R. L. Portsmouth, *J. Non-Cryst. Solids* **150**, 69–95 (1992).
- [5] S. R. Elliott, *Nature (London)* **354**, 445 (1991); *Phys. Rev. Lett.* **67**, 711–714 (1991); *J. Phys. Condens. Matter* **4**, 7661–7678 (1992).
- [6] L. F. Gladden, *J. Non-Cryst. Solids* **119**, 318–330 (1990); in *The Physics of Non-Crystalline Solids*, edited by L. D. Pye, W. C. LaCourse, and H. J. Stevens (Taylor & Francis, London, Washington, 1992), pp. 91–95.
- [7] J. D. Wicks, Ph.D. thesis, Oxford, 1993.
- [8] A. C. Wright [*J. Non-Cryst. Solids* **179**, 84–115 (1994)] has shown that the residual discrepancy between model and experimental neutron scattering data is about 2% for the best of Gladden’s models—significantly better than most atomic models for silica.
- [9] R. Alben, G. S. Cargill III, and J. Wenzel, *Phys. Rev. B* **13**, 835–42 (1976).
- [10] P. H. Gaskell, in *Proceedings of a One-Day Meeting of the Electron Microscopy and Analysis Group of the Institute of Physics*, edited by K. M. Knowles (Cambridge University, Cambridge, 1988), Vol. 11, pp. 47–58.
- [11] Distorted “planar” atomic density fluctuations with spacing  $2\pi/Q_1$  could also reproduce the *orientationally-averaged* FSDP. We do not exclude multiply twinned, polytetrahedral, or “curved-space” models [see, for example, D. Turnbull, *J. Chem. Phys.* **20**, 411–424 (1952); D. R. Nelson and F. Spaepen, in *Solid State Physics*, edited by H. Ehrenreich and D. Turnbull (Academic Press, New York, 1989), Vol. 42, p. 190]—or even “allianceous” (onionlike) structures.
- [12] P. S. Salmon, *Proc. R. Soc. London A* **445**, 351–366 (1994).
- [13] A. Uhlherr and S. R. Elliott, *J. Phys. Condens. Matter* **6**, L99–L105 (1994).
- [14] D. I. Grimley, A. C. Wright, and R. N. Sinclair, *J. Non-Cryst. Solids* **119**, 49–54 (1990).